Table of Contents

Chapter 1

Introduction

Never a dull moment. Not in the field of optoelectronics; not since the merging of semiconductors and optics was cemented some half century ago after Chapin and colleagues at Bell Labs made practical use of the photovoltaic effect in a silicon solar cell [1]. And of the many defining moments in optoelectronics research, perhaps paramount of them all was the first observations in 1962 by Hall *et al.* [2] and Holonyak *et al.* [3] of stimulated emission in electrically pumped semiconductors. Since that time, optoelectronic technology has become an integral part of our daily lives. Solar cells may well be on the verge of contributing to the elimination of fossil fuels. Light emitting diodes (LEDs) are rapidly replacing Edison's incandescent bulb. How many liquid crystal display (LCD) devices do you own... too many to count in a single attempt?

Semiconductor laser technology is no different. Without these lasers, our telecommunications pipelines would be vastly less efficient. We would be relying on the same technology that powered Henry's electromagnetic telegraph: electrons traveling through wire (slow) rather than photons traveling through glass (fast!). Today's semiconductor lasers, and indeed to varying degrees most all optoelectronic devices, make use of a fundamental concept dubbed heterostructure engineering. In fact, the heterostructure's ubiquity was recognized by the year 2000 Nobel prize in physics, awarded to Zhores Alferov [4] and Herbert Krömer [5] for their pioneering work. A heterostructure device is composed of layers of different materials, overlayed one after the other. These layers are strategically selected and used to precisely control how electrons—*i.e.* current—pass through a device.

The layers that make up a heterostructure can be made exceedingly thin: thicknesses on the order of a single atomic layer. The ability to form such thin layers make heterostructures one of man's ultimate engineering conquests of quantum mechanics. Just as nature's atom puts electrons into discrete energy orbits, man's quantum-confined heterostructure forces electrons into discrete energy states as they pass through a heterostructure device. By exploiting this ability, we can influence when, where, and how electrons interact with their surroundings. In the seminal work that first recognized this possibility of quantum confinement in heterostructures, Esaki and Tsu in 1970 theorized that a particular heterostructure implementation could result in *negative* resistance at certain applied voltage levels [6]. The following year, Kazarinov and Suris proposed that the man-made energy states of quantum-confined heterostructures could be used as the basic optical transition for a new type of laser [7]. Despite multiple attempts it took some 25 years to realize such an intersubband heterostructure laser [8], now known as the quantum cascade (QC) laser. The year 2009 marks the 15th anniversary of the first reported QC laser demonstration.

The genius of the heterostructure concept—and the quantum cascade in particular—lies in its innate engineerability. In this thesis, I hope to convey how the QC concept provides vast opportunity for creative new ideas that can expand technological capabilities and improve device performance.

1.1 Engineered Mid-infrared Light Sources: Present and Future

QC lasers are particularly suited for generating light at mid-infrared (mid-IR) wavelengths. Loosely defined, the mid-infrared is the spectral region between 3 and 30 μm in wavelength (10–100 THz in frequency). As illustrated in Fig. 1.1, these boundaries mark convenient transitions between the capabilities of three different technologies that are today's most capable electrically-pumped semiconductor-based laser sources. From the visible region to about 3 μm diode lasers dominate [4] [5]; diode lasers are especially capable at the 0.98 and 1.55 μm "telecom" bands. On the long wavelength side, THz QC lasers are the dominant injection laser technology [9]. Although Pb-salt diode lasers were once the best option for mid-infrared injection sources, QC lasers have emerged as

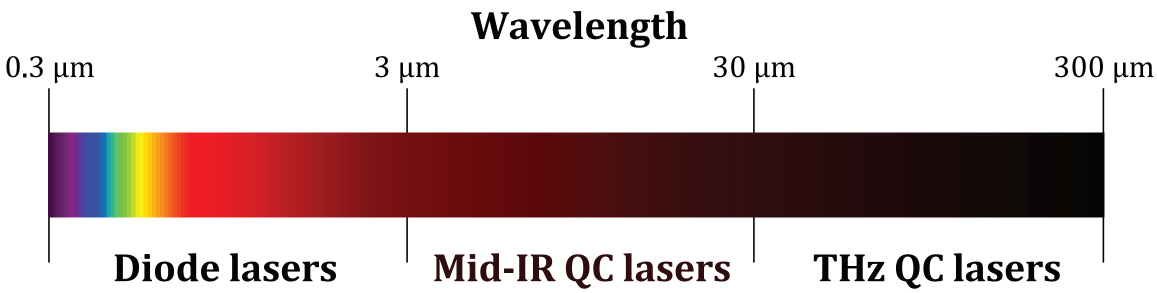

Figure 1.1: The electromagnetic spectrum. The wavelengths from 0.3 to 300 μm are covered by three semiconductor laser technologies. The mid-infrared, loosely defined as 3 to 30 μm, is the regime of mid-infrared QC lasers. Between the transitions for laser device types—diode–to–mid-IR QC laser and mid-IR QC laser–to–THz QC laser—lie spectral gaps of substantial technical challenge. The first gap, explored in Chapter 3, results from fundamental loss mechanisms in diode lasers and band offset limitations in mid-IR QC lasers. The second gap, explored in Chapter 4, derives fundamentally from the semiconductor restrahlen band in the 30–60 μm region.

far more capable devices. Mid-infrared QC lasers span 2.75 μm [10] to 24 μm [11], with various performance levels in between. In general, room temperature (RT), continuous wave (CW) lasing is now the technological standard from 4–12 μm.

An ability to easily generate mid-infrared light is most certainly of technological importance. Holding a wide swath of the electromagnetic spectrum, mid-infrared light can be exploited for unique applications. While there are numerous applications for mid-infrared light, with more surely on the horizon, here I briefly discuss just three examples: defense countermeasures, open atmosphere data transmission, and molecular species detection.

1.1.1 Defense countermeasures

Deployable flares, such as those being emitted from an AC-130U gunship in Fig. 1.2, are the conventional countermeasure against IR-guided (heat-seeking) missiles. Modern infrared countermeasures (IRCMs), which use directed infrared light sources to “jam” the targeting system on an IR-guided missile—in effect blinding the missile, have qualities that make them far more effective by comparison. The ability to highly tailor the spectral signature and modulation properties of a light source is a key advantage over older flare-based technologies. Modern IRCMs also do not require an aircraft to

Figure 1.2: Infrared countermeasure flares deployed from an AC-130U gunship. An AC-130U gunship jettisons flares over an area near Hurlburt Field, Florida. The flares are a decoy for heat-seeking missiles that may be fired at the aircraft. The aircraft is from the 4th Special Operations Squadron. Courtesy of the U.S. Air Force [12].

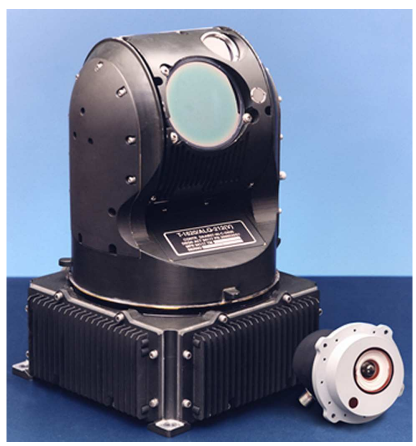

Figure 1.3: IRCM module. An early photo of Lockheed Martin's ATIRCM. Courtesy of BAE Systems press release [13].

undergo "evasive maneuvers" to physically separate itself from dropped flares. As a craft-mountable module, shown in Fig. 1.3, these systems couple threat identification and tracking together with targeting and jamming into a system that does not require expendable components such as flares.

The two modern IRCM programs, Northrup Grumman's NEMESIS Directional Infrared Countermeasure (DIRCM) and Lockheed Martin's Advanced Threat Infrared Countermeasures (ATIRCM), both use solid state laser light sources. These are bulky, only operate under pulsed conditions, and have spectral emission characteristics that are difficult to

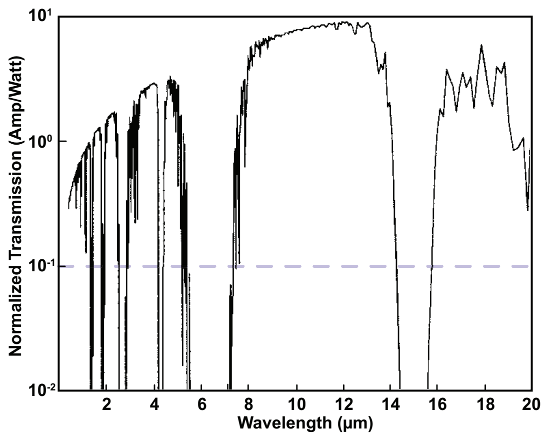

(a)

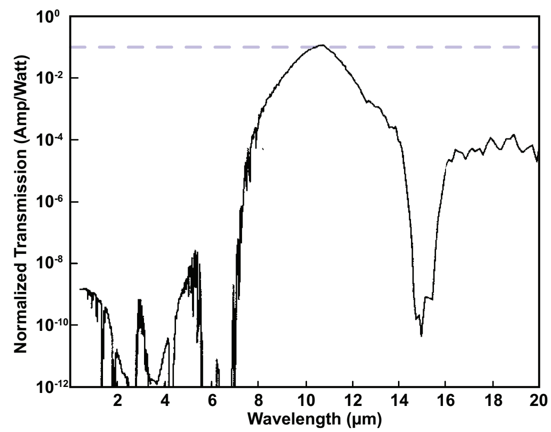

(b)

Figure 1.4: Atmospheric absorption versus wavelength. Mid-infrared wavelengths, especially in the second atmospheric window near 10 μm, are considerably more "clear" during adverse weather. Panel (a) shows transmission for very clear weather ("visibility," 50 km) while (b) shows transmission for thick fog ("visibility," 200 m). The dashed line represents normalized transmission at 10^{-1} A/W for comparison. Reprinted from [14] with permission from the Optical Society of America.

customize. By comparison, QC lasers are miniature devices, capable of CW operation, and have spectral emission that is highly configurable. Clearly, QC lasers are of interest to replace and improve upon the present-day IRCM light sources.

1.1.2 Open atmosphere data transmission

Methods for transmitting information through the atmosphere, and specifically free space optical communications systems, use laser-based transceivers for line-of-site data transmission. Compared to other communications technologies, free space optical communications combines capabilities of extremely high bandwidth, rapid deployment time, and license- and tariff-free bandwidth allocation. The major weakness of free space optical communications is the threat of sporadic downtime associated with adverse weather conditions such as fog, haze, or rain that prevent the signal (light) from propagating through the atmosphere. The wavelength-dependence of atmospheric absorption for clear and foggy conditions is shown in Fig. 1.4, as calculated by Manor and Arnon [14]. For clear weather, the advanced capabilities of telecom lasers around

1.5 μm would certainly suffice. Yet under adverse conditions, as shown in Fig. 1.4b, transmission near 1.5 μm decreases by approximately 9 orders of magnitude. In comparison, transmission for 10 μm light only decreases by 2 orders of magnitude between the two atmospheric conditions, and the difference between 1.5 μm light on a clear day and 10 μm light on a foggy day is only 1 order of magnitude. The mid-infrared is a most convenient wavelength for applications where atmospheric transmission is important, free space optical communications included.

1.1.3 Molecular species detection

Perhaps the most versatile of the applications for mid-infrared light is its use in the detection of trace molecules. Molecular detection based on sensing the presence of light absorption can be versatile, selective, and sensitive [15]. Individual molecular species have unique energies at which they absorb light, the absorption energies corresponding to vibrational and rotational modes of the molecule. Figure 1.5 shows absorption spectra for several common and important atmospheric gasses. These molecule-specific absorption "fingerprints" can be used to selectively determine the presence of a particular species, including isotropic ratios, by an absorption spectroscopy system. Such a system typically has three components: a light source, a light-matter interaction space, and an optical detector. For gas-phase absorption spectroscopy, the light source wavelength is tuned to correspond to an absorption line of a targeted molecular species, the light is allowed to interact with a gas sample in a cavity such as a Herriot cell, and the remaining light is collected on an optical detector. All else being equal, maximum sensitivity is achieved when the frequency of the light source is selected to be on resonance with the strongest absorption line of the target species. That is, the use of fundamental mode absorption resonances, most typically at mid-infrared wavelengths, will yield the most effective and sensitive detection systems.

1.2 Quantum Cascade Lasers

Understanding the basic operation of a QC laser most easily starts by comparison with the more well-known diode laser. QC lasers and diode lasers share several common elements. Both are semiconductor injection lasers; that is, they employ "top" and

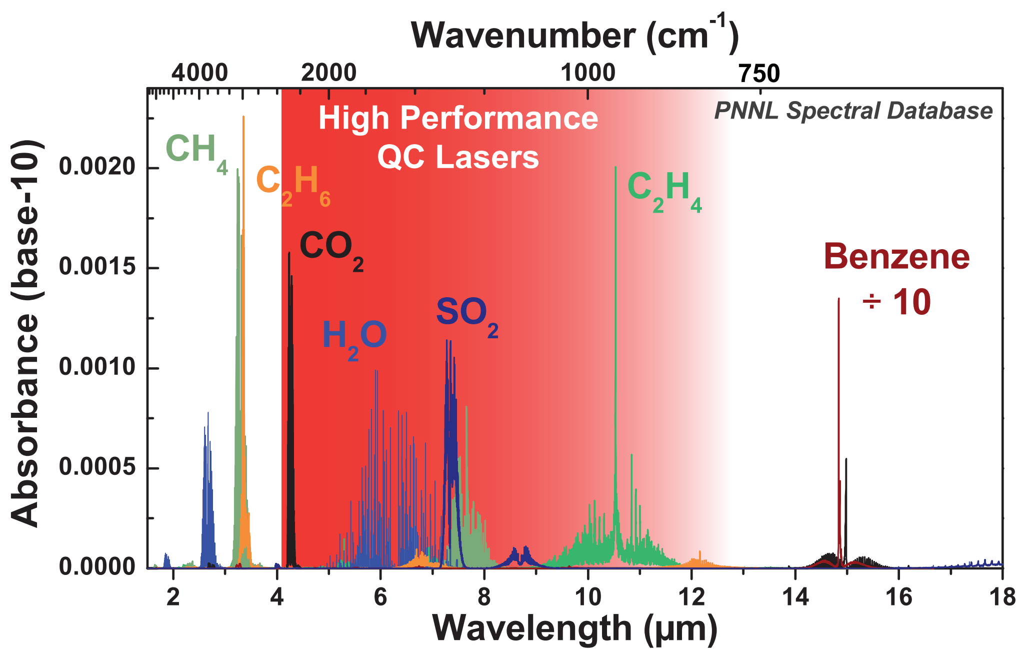

Figure 1.5: Spectral absorption signatures for several atmospheric gasses. Most molecular species have their fundamental resonances at wavelengths beyond 3 μm, out of reach of diode lasers. High performance (RT CW) QC lasers are able to cover a large many of the resonances of interest.

"bottom" metal contacts that allow electric current to be pumped through the device. Both laser types make use of similar dielectric waveguide structures, where an optical mode is designed to tightly overlap with a semiconductor region that provides optical gain.

Beyond these characteristics, differences start to emerge. The fundamental mechanics by which diode lasers and QC structures generate light are different. In diode lasers, electrons combine with holes across the fundamental semiconductor bandgap to produce photons at the bandgap energy. Thus a key device property, the emission wavelength, is set by the semiconductor material itself. QC lasers, by contrast, use coupled quantum wells to tailor nearly every aspect of the device properties. Figure 1.6 pictorially shows a QC laser's energy band structure. The positions of each individual energy state are uniquely determined by the selection of well and barrier widths.

A QC laser's design can be divided into two sections: the active regions and the injector regions. QC active regions have at least three important energy "states," which

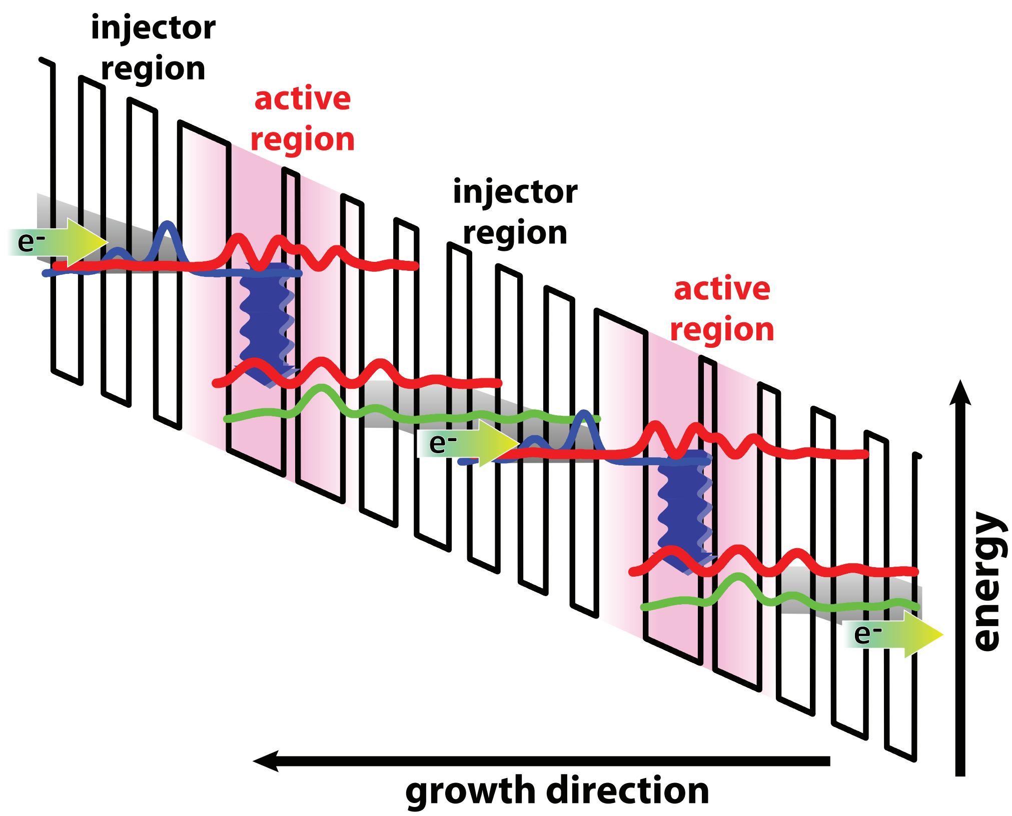

Figure 1.6: Basic QC laser band diagram. The conduction band edge of the alternating wide and narrow bandgap materials are is shown, along with the stationary wavefunctions of the quantum wells. QC lasers have an active region, where optical transitions are engineered to occur, and an injector region, which stitches together successively "cascaded" active regions. When a sufficient electric field is applied, indicated in the figure by the constant slope, electrons are able to transit through the entire QC structure.

are in fact energy sub-bands. Two states are needed to form the upper and lower energy states of the optical transition. The positions of these states are selected to give an energy separation of the desired photon energy, and they are usually designed to have large overlap integrals to yield a large oscillator strength. A third important active region state is placed below the lower laser state; an energy separation of at least one longitudinal optical (LO) phonon is used. LO phonons represent the fastest electron scattering mechanism in semiconductors. This lowest energy state is thus intended to quickly empty the lower energy level, and hence for the first two states provide an in-built population inversion.

The other important QC laser section is the QC injector region. QC injectors do all of the important functions necessary to "stitch together" consecutive active regions. That is, QC injectors impart the ability to take electrons from the lower states in one active region and inject them into the upper laser state of the next, down-stream active region. Through this stitching together of multiple active–injector region periods, multiple photons are emitted for each single electron that passes through the structure. A detailed examination of the role of injector regions is given in Chapter 5.

1.2.1 Current Capabilities

Wavelength range: 4.2 Ű 12 ţm

Wall-plug efficiency: ? 20

usually « 20

Single spectral mode, single spatial mode

Low-input power, low-output power devices

Long operating lifetimes

TheyŠre light weight!

1.2.2 Current Challenges

1.3 The QC Development Process

1.3.1 Design

Cite: Claire Nature broadband [16], Capasso Raman [17], Faist double phonon [18], Faist bloch gain [19], Scamarcio superlattice [20]

Laser design is the first step in the development of a QC laser. Because of the high configurability of QC structures, design is a crucial element that determines laser performance.

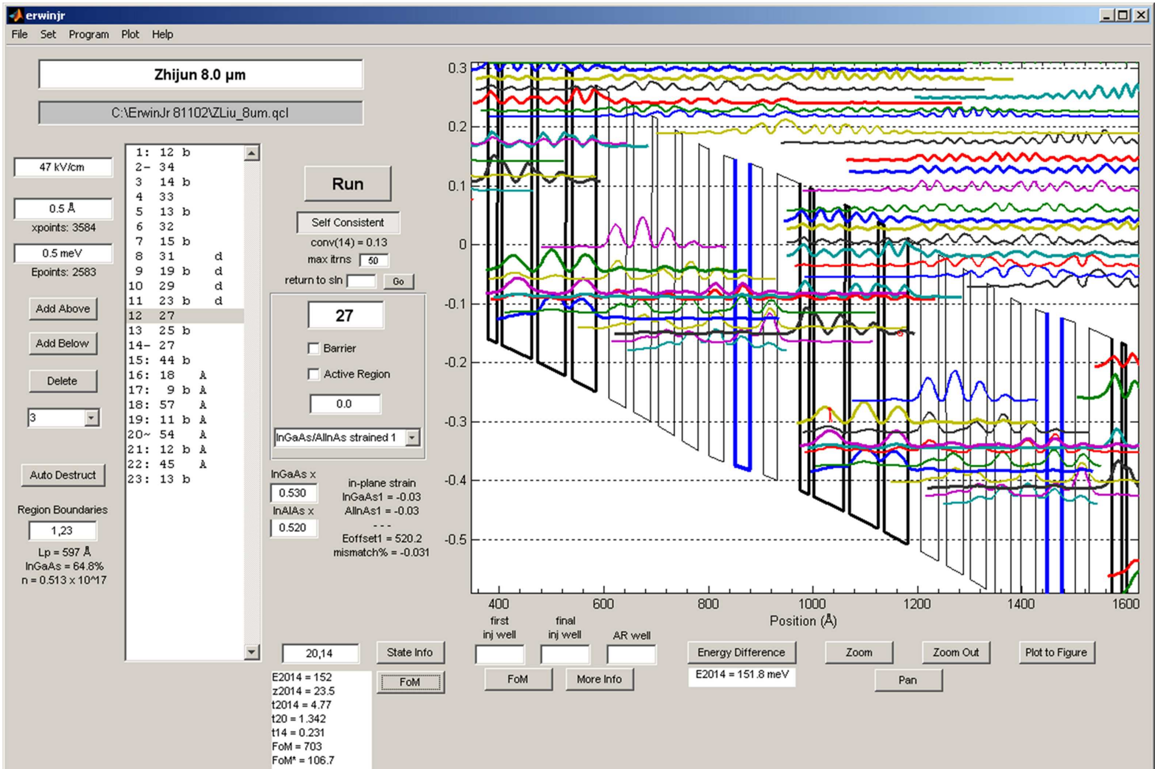

Figure 1.7: Example use of the shooting method. The left panel shows a potential $V(z)$ for an $In_{0.53}Ga_{0.47}As$ / $Al_{0.48}In_{0.52}As$ quantum well with $E_{field} = 25$ kV/cm. Four bound solutions are found by finding the roots of $\psi(z_{end})$, as shown in the right panel. The wavefunction $\psi(z)$ is plotted for the four bound solutions.

1.3.2 Growth

1.3.3 Fabrication

1.4 Thesis Overview

This thesis seeks to demonstrate the power of the quantum cascade as a flexible device technology platform. Never before has a laser system afforded engineers so much control over its fundamental, internal mechanisms. Truly, the QC concept imparts the unprecedented ability to create new device architectures that incorporate new operation concepts. Throughout this thesis, we provide examples of how this flexibility can be exploited to improve device performance and expand device capabilities.

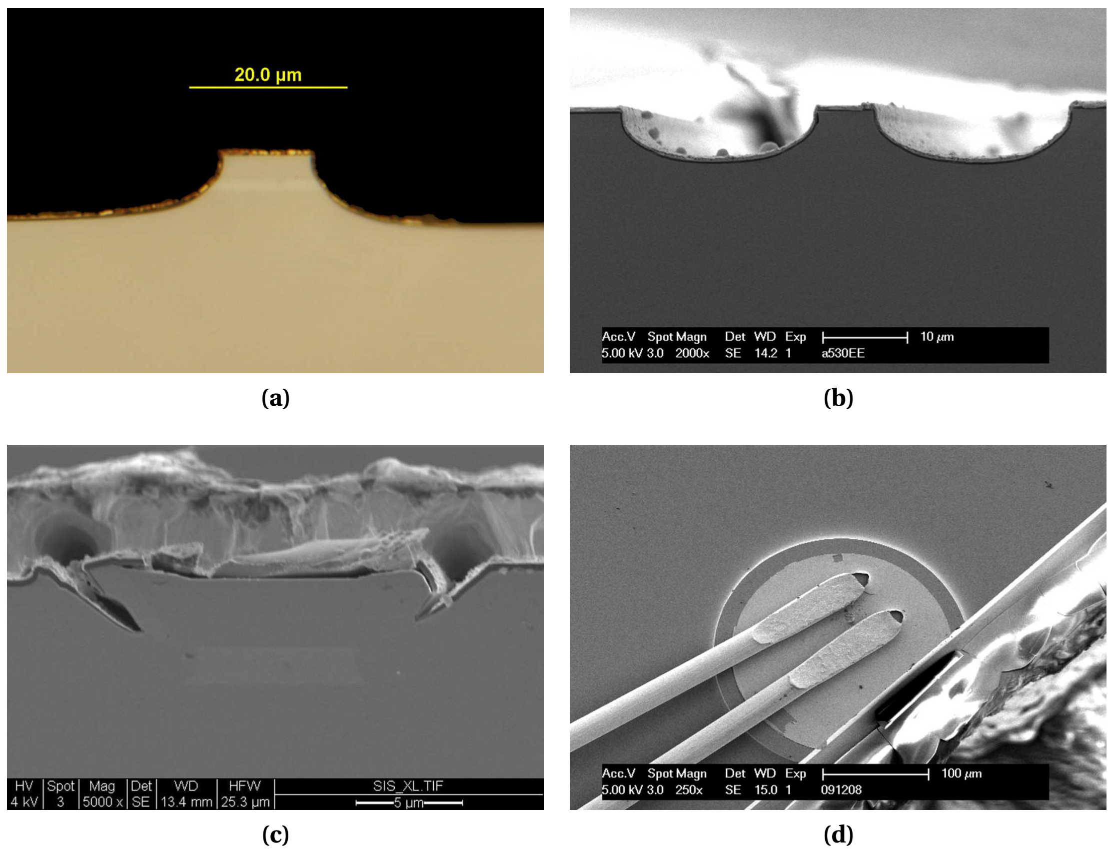

Figure 1.8: Energy band diagrams for the three injector well QC structure. The as-designed turn-on field is 114 kV/cm, shown here in (a). According to EL data, current transport begins at a field of 85 kV/cm, shown in (b). Electron transport leading to negative differential resistance is also observed starting at 95 kV/cm, shown in (c). At 95 kV/cm the second energy level of one active region is in resonance with the down-stream upper laser state at this field.

In Chapter 2, we provide a theoretical foundation for basic operation principles of QC lasers. Key tools used in laser design, such as accurate solutions to the Schrödinger equation and the optical dipole matrix element, are explicitly discussed. Derivations for important device performance parameters, such as threshold current and wall-plug efficiency, are given with sufficient detail to clearly understand the origins and contributions of important design parameters.

As an example of the flexibility of the technology platform, Chapter 3 discusses implementing QC structures in an entirely new materials system: ZnCdSe / ZnCdMgSe [21]. This II–VI materials system has some properties that may be advantageous over the currently used III–V materials system, such as larger conduction band offsets, which ultimately may be useful for developing shorter wavelength QC lasers than those currently available.

In contrast, the motivation for Chapter 4 starts with expanding the capabilities of QC lasers on the long wavelength side. Here, we present a new QC architecture—one which employs optical transitions made completely of quantum well excited states [22]. These excited state structures have the ability to compensate for many of the deleterious factors that make long-wavelength lasing so difficult. Through experimenting with this new structure, we found the unexpected and unique property of lasing high in k-space [23].

Chapter 5 presents a fundamental re-examination of the role of QC injector regions. Since the injector regions are not the source of photons, they can in some ways be viewed as "wasted space." However, injector regions practically serve several functions that are crucial to high laser performance. Here, we look at minimizing injector length, and we employ QC designs that drastically reduce the overall period length of the structure. Like in the results of Chapter 4, we observe unique and unexpected properties. These observations allow us to draw new insights into and understanding of fundamental QC laser operation mechanisms.

Finally, concluding remarks are given in Chapter 6, along with an outlook for the future of QC technology.

References

[1] D. M. Chapin, C. S. Fuller, and G. L. Pearson, "A New Silicon p-n Junction Photocell for Converting Solar Radiation into Electrical Power," *J. Appl. Phys.* **25**, 676 (1954). doi:10.1063/1.1721711

[2] R. N. Hall, G. E. Fenner, J. D. Kingsley, T. J. Soltys, and R. O. Carlson, "Coherent Light Emission From GaAs Junctions," *Phys. Rev. Lett.* **9**, 366 (1962). doi:10.1103/PhysRevLett.9.366

[3] J. Nick Holonyak and S. F. Bevacqua, "Coherent (Visible) Light Emission from Ga($As_{1-x}P_x$) Junctions," *Appl. Phys. Lett.* **1**, 82 (1962). doi:10.1063/1.1753706

[4] Z. I. Alferov, "The double heterostructure concept and its applications in physics, electronics, and technology," *Rev. Mod. Phys.* **73**, 767 (2001). doi:10.1103/RevModPhys.73.767

[5] H. Kroemer, "Quasielectric fields and band offsets: teaching electrons new tricks," *Rev. Mod. Phys.* **73**, 783 (2001). doi:10.1103/RevModPhys.73.783

[6] L. Esaki and R. Tsu, "Superlattice and Negative Differential Conductivity in Semiconductors," *IBM J. Res. Dev.* **14**, 61 (1970). url: http://www.research.ibm.com/journal/rd/141/ibmrd1401H.pdf

[7] R. F. Kazarinov and R. A. Suris, "Possibility of Amplification of Electromagnetic Waves in a Semiconductor with a Superlattice," *Sov. Phys. Semicond.* **5**, 207 (1971).

[8] J. Faist, F. Capasso, D. L. Sivco, C. Sirtori, A. L. Hutchinson, and A. Y. Cho, "Quantum Cascade Laser," *Science* **264**, 553 (1994). doi:10.1126/science.264.5158.553

[9] B. S. Williams, "Terahertz quantum-cascade lasers," *Nature Photonics* **1**, 517 (2007).
doi:10.1038/nphoton.2007.166

[10] J. Devenson, O. Cathabard, R. Teissier, and A. N. Baranov, "InAs/AlSb quantum cascade lasers emitting at 2.75–2.97 µm," *Appl. Phys. Lett.* **91**, 251102 (2007).
doi:10.1063/1.2825284

[11] R. Colombelli, F. Capasso, C. Gmachl, A. L. Hutchinson, D. L. Sivco, A. Tredicucci, M. C. Wanke, A. M. Sergent, and A. Y. Cho, "Far-infrared surface–plasmon quantum–cascade lasers at 21.5 µm and 24 µm wavelengths," *Appl. Phys. Lett.* **78**, 2620 (2001).
doi:10.1063/1.1367304

[12] Senior Airman Julianne Showalter, *United States Air Force*

[13] BAE Systems, "BAE SYSTEMS' ATIRCM/CMWS Successfully Completes Army Live-fire Tests; Key Testing Milestone Accomplished," *Press Release* (May 15, 2001).

[14] H. Manor and S. Arnon, "Performance of an Optical Wireless Communication System as a Function of Wavelength," *Appl. Opt.* **42**, 4285 (2003).
doi:10.1364/AO.42.004285

[15] A. A. Kosterev, R. F. Curl, F. K. Tittel, M. Rochat, D. Hofstetter, and J. Faist, "Chemical sensing with pulsed QC–DFB lasers operating at 15.6 µm," *Appl. Phys. B* **75**, 351 (2002).
doi:10.1007/s00340-002-0963-z

[16] C. Gmachl, D. L. Sivco, R. Colombelli, F. Capasso, and A. Y. Cho, "Ultra-broadband semiconductor laser," *Nature* **415**, 883 (2002).
doi:10.1038/415883a

[17] M. Troccoli, A. Belyanin, F. Capasso, E. Cubukcu, D. L. Sivco, and A. Y. Cho, "Raman injection laser," *Nature* **433**, 845 (2005).
doi:10.1038/nature03330

[18] M. Beck, D. Hofstetter, T. Aellen, J. Faist, U. Oesterle, M. Ilegems, E. Gini, and H. Melchior, "Continuous Wave Operation of a Mid-Infrared Semiconductor Laser at Room Temperature," *Science* **295**, 301 (2002).
doi:10.1126/science.1066408

[19] R. Terazzi, T. Gresch, M. Giovannini, N. Hoyler, N. Sekine, and J. Faist, "Bloch gain in quantum cascade lasers," *Nature Physics* **3**, 329 (2007).
doi:10.1038/nphys577

[20] G. Scamarcio, F. Capasso, C. Sirtori, J. Faist, A. L. Hutchinson, D. L. Sivco, and A. Y. Cho, "High-Power Infrared (8-Micrometer Wavelength) Superlattice Lasers," *Science* **276**, 773 (1997).
doi:10.1126/science.276.5313.773

[21] K. J. Franz, W. O. Charles, A. Shen, A. J. Hoffman, M. C. Tamargo, and C. Gmachl, "ZnCdSe/ZnCdMgSe quantum cascade electroluminescence," *Appl. Phys. Lett.* **92**, 121105 (2008).
doi:10.1063/1.2903135

[22] K. J. Franz, D. Wasserman, A. J. Hoffman, D. C. Jangraw, K.-T. Shiu, S. R. Forrest, and C. Gmachl, "Evidence of cascaded emission in a dual-wavelength quantum cascade laser," *Appl. Phys. Lett.* **90**, 091104 (2007).
doi:10.1063/1.2709970

[23] K. J. Franz, S. Menzel, A. J. Hoffman, D. Wasserman, J. W. Cockburn, and C. Gmachl, "High k-space lasing in a dual-wavelength quantum cascade laser," *Nature Photonics* **3**, 50 (2008).
doi:10.1038/nphoton.2008.250